Journal of Cultural Heritage 78 (2026) 45–54

Contents lists available at ScienceDirect

Journal of Cultural Heritage

journal homepage: www.elsevier.com/locate/culher

VSI: TECHNART 2025

Shining a light on the degradation of triarylmethane dyes: Multi-analytical study of a faded 1880s printed cotton dress

Catarina M. Pinto[a,*], David Buti[b], Letizia Monico[a,c], Aldo Romani[c], Lucia Burgio[d], Brenda Doherty[a,*]

[a] CNR, Institute of Chemical Science and Technologies "G. Natta" (SCITEC), Perugia, Italy
[b] CNR, Institute of Heritage Science (ISPC), Florence, Italy
[c] SMAArt Centre of Excellence and University of Perugia, Department of Chemistry, Biology and Biotechnology, Perugia, Italy
[d] Science Section, Conservation Department, Collections Care and Access, Victoria and Albert Museum, Cromwell Road, South Kensington, London SW7 2RL, UK

ARTICLE INFO

Article history:
Received 28 July 2025
Accepted 8 January 2026
Available online 23 January 2026

Keywords:
Triarylmethane dyes
Printed dress
Photodegradation
Benzophenone

ABSTRACT

This study examines the fading of the blue-green background in an 1885 printed cotton dress by Edmund Potter & Co., in the collection of the Victoria and Albert Museum (V&A). Uneven fading patterns indicate differential light exposure, with protected areas retaining greater vibrancy. An in-situ analytical campaign employing portable UV–VIS–NIR spectroscopy, colorimetry, and VIS hyperspectral imaging identified dye constituents and evaluated their conservation state. Complementary micro-destructive Surface Enhanced Raman spectroscopy suggests the presence of early synthetic triarylmethane dyes. To further investigate their photo-fading behaviour, mordanted cotton mock-ups dyed with selected blue-green triarylmethane dyes commercially available at the time of the dress's production, namely, diamond green B (C.I. 42,000, Basic Green 4, 1877), diamond green G (C.I. 42,040, Basic Green 1, 1879) and yellowish light green SF (C.I. 42,095, Acid Green 5, late 19th Century) were subjected to controlled aging and monitored. Comparative analysis with in situ data provided contextual insight into the photochemical behaviour of the dyes, highlighting differences associated with substituent type and orientation and their potential influence on observed photoproducts, including benzophenones. These findings advance the understanding of triarylmethane dye fading in important historical textiles and inform conservation strategies for museum display of such dye sensitive collections.

Introduction and research aim

Triarylmethane dyes (TAMs) are renowned for their versatile vivid hues from red and purple to blue and green and cost-efficient production, which led to their rapid industrial adoption following their commercialization in the 1880s. Within the context of heritage science, TAMs are of particular importance due to their extensive historical use in textile dyeing and printing. Beyond textiles, they were also widely employed in cosmetics, biological stains, printing, ballpoint pens, and writing inks [1–3]. Since the 17th century, textile printing in Europe was driven by advancements in design, production and dyers' chemical expertise whose, with the advent of synthetic dyes, further transformed the industry [4–6]. Calico printing transformed the textile industry by enabling precise application of dyes to create patterned fabrics. Edmund Potter (1802–1883) advanced this technique, making his Dinting Vale Works (UK) a global leader. Texts from that time emphasised that Potter's 'design library' and colour lab actually drove innovation, earning recognition for unique Victorian patterns [7]. To afford a great variety of shades and strength, since 1880s, the triarylmethane family dyes were actively used for printing [8].

Structurally, TAM dyes observe a common chemical backbone with three conjugated aromatic rings attached to a central carbon atom[1] differing in their various auxochromic substituents (Fig. 1). However, TAMs notably observe a low lightfastness (ISO 2) [9] and are susceptible to fading when exposed to light and oxygen. Their environmental impact and toxicity and subsequent effort for their efficient chemical breakdown and removal from wastewaters has provided motivation in recent decades for the studies to elucidate their complex photodegradation pathways. TAMs undergo different degradation mechanisms and reaction pathways also depending on the orientation of substituents, thus leading to specific degradation

* Corresponding authors.
E-mail addresses: catarinamonteiropinto@cnr.it (C.M. Pinto), brenda.doherty@cnr.it (B. Doherty).

https://doi.org/10.1016/j.culher.2026.01.008

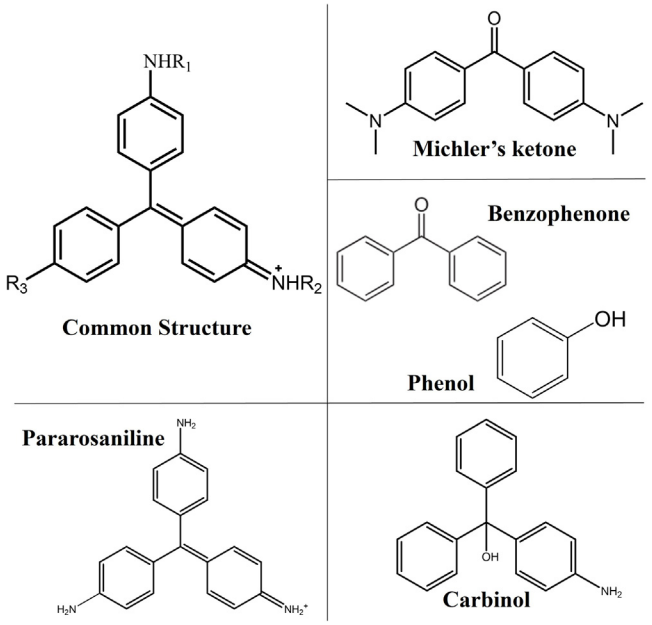

Fig. 1. Triarylmethane dyes backbone and main elucidated photoproducts through several oxidative degradation pathways in literature [3,17,18].

rates and colour fading. Light exposure is noted in literature to provoke several degradation pathways including: *N-dealkylation*, where methyl groups on the dye are sequentially replaced by hydrogen atoms[10]; *photo-oxidative cleavage* of the central C-phenyl bond[11]; *ring opening* initiated by hydroxyl radicals (•OH) generated from singlet oxygen in water[3]; and *photo-reduction* of the excited dye cation to its *leuco* form, either by electron addition to the photoexcited species or by photochemical hydrogenation [12]. In cultural heritage materials, the conditions in which dyes are found influence their photochemical behaviour and, consequently, their degradation processes [13]. For example, literature notes that the use of fillers such as titanium dioxide in high-quality paper can affect the rate of N-dealkylation [14]. N-dealkylation has also been reported in powder samples [15] while, on the other hand, photo-oxidative processes are observed when dyes are present alongside binders [16].

These degradation pathways often compete, rendering the process highly complex also significantly affected by external factors such as heat, light intensity, wavelength, and humidity. Photodegradation of TAMs typically produces oxidation products such as quinone-like compounds and benzophenone derivatives, along with dealkylated species. Hydroxylated products, aromatic amines, and carbonyl compounds are also formed due to cleavage and oxidation of the molecular structure. Prolonged light exposure can yield smaller fragmentation products, such as organic acids and aldehydes [19]. These photoproducts, identified via spectroscopy and chromatography, reflect the varied chemical pathways of oxidation, N-dealkylation, and molecular breakdown under light exposure. Fig. 1 shows the common molecular structure of triarylmethanes alongside frequently reported photoproducts: Michler's ketone, benzophenone, and phenol from photo-oxidative cleavage; pararosaniline from N-dealkylation; and carbinol from hydrolysis) [2,17,18,20–24].

Over the past decades, analytical techniques have been employed to investigate this class of dyes, predominantly in solution and in historical artifacts as colorants, inks and dyes due to their chemical complexity, historical significance, and relevance for conservation employing namely UV–VIS–NIR spectroscopy, Infrared and Raman/Surface-Enhanced Raman Scattering (SERS) techniques [2,20,18,22,25–27]. Micro-destructive chromatographic methods have been utilised including, HPLC-DAD-ESI-Q-ToF, LC-MS and LC-MS-MS favouring the identification of degradation products [3,28,29]. More recently, pyrolysis coupled with GC–MS, and capillary electrophoresis [30] and UHPLC-PDA-HRMS have been employed emphasising the complexity and diverse compositions of dye production to gain a better understanding of the formulation of historical drawings and manuscripts inks [15]. Integrating these findings is key to elucidating the chemical behaviour of triarylmethane dyes in varied matrices, a requirement increasingly vital to the field of cultural heritage preservation. To understand the fading phenomena observed in the historical Edmund Potter & Co cotton dress and ultimately inform its preservation, an in-situ analytical campaign was carried out, supported by a controlled photo-aging study on textile mock-ups. The mock-ups provide a controlled setting to better elucidate the synthetic dyestuff and the processes driving its photodegradation, which helps interpret changes in the original textile. Based on the production timeline of the dress, dated about 1885, and through preliminary micro-destructive analytical investigations of a micro-sample collected during a recent conservation intervention (2023), it is hypothesised that early synthetic dyes from the triarylmethane family were employed in the now faded background coloration. The in-situ campaign outcomes were used to construct a series of mordanted cotton textiles to examine the photo-fading behaviour of selected blue-green triarylmethane dyes. The selection of these dyes was based on their class, colorimetric data, production year (which needed to precede the dress's production date), and their reflectance spectra. Based on these criteria, three dyes from our database were chosen: Diamond Green B (DGB), Diamond Green G (DGG), and Yellow Light Green S.F (YLG). The mordanted cotton mock-ups were subjected to analytical monitoring by non-invasive and micro-invasive techniques, including UV–VIS–NIR spectroscopies and colorimetry. The resulting analytical data are compared with those collected in-situ. These findings may support colour reconstruction efforts and assist in defining a coherent scientific predictive basis to contribute to the optimization of preventive conservation strategies of historical artifacts utilising analogous TAM dye systems.

Material and methods

Materials

Dress: The V&A houses an exemplary printed cotton dress by Edmund Potter & Co, Fig. 2.a. This textile design, influenced by Japanese kamon circular emblems, reflects the impact of Japanese art on late Victorian design [31]. The dyes used are undocumented and the garment exhibits a blue-green background, with evident signs of fading in areas not shielded from direct light exposure, such as beneath flaps and overlaps of the bodice which remain still more brightly coloured (see details of Fig. 2.b).

Textile mock ups preparation: Raw cotton was dyed with selected triarylmethane dyes fitting of the turquoise colour in the dress which were commercialised at the time of its manufacture, namely, DGB (Basic Green 4, C.I. 42,000), DGG (Basic Green 1, C.I. 42,040) and YLG (Acid Green 5, C.I. 42,095), Fig. 3. Raw cotton was mordanted with gallic acid [32] using a simplified method, a 100:6 (cotton:mordant, w/w) ratio by pre-soaking for 2 h, dissolving gallic acid in hot water, and treating the fibres for 1 h at 70 – 80 °C. Dye method: For the basic dyes (DGB and DGG), 20 mg of dye were dissolved in 150 mL of demineralised water at 70 °C. Cotton fabric (2 g; 2.5 × 16.5 cm) was immersed in the dye bath and held at 70 °C for 30 min, with stirring every 5 min. The samples were cooled in the bath and rinsed with demineralised water.

Fig. 2. Image of **a**) printed cotton dress and **b**) details of fading of the blue background [printed by Edmund Potter & Co. (1885, made), Accession Number T.7–1926]. © Victoria and Albert Museum.

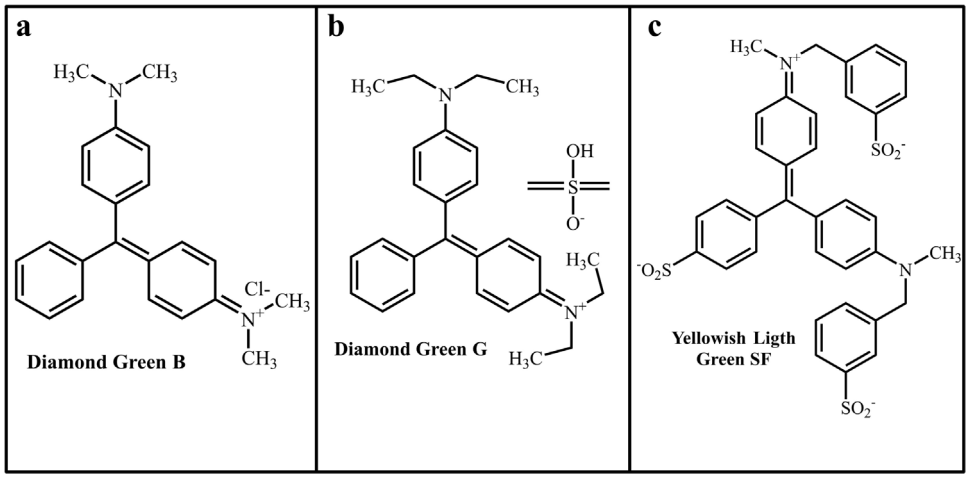

Fig. 3. Molecular structures of **a**) diamond green B (DGB), **b**) diamond green G (DGG) and **c**) yellowish light green SF (YLG).

For the acid dye (Yellowish Light Green SF), 150 mL of demineralised water was heated to 70 °C, 10 g sodium sulfate and 30 mg dye were added, and the cotton sample (2 g) was immersed. After adding 40 µL concentrated sulfuric acid, dyeing proceeded at 70 °C for 30 min with periodic stirring. The fabric was cooled in the bath and rinsed with demineralised water.

Artificial Ageing: Photoaging experiment were performed using an ozone free Cermax xenon lamp filtered by water and UV filter (> 400 nm) at different step of irradiation time, over 203 h. Light irradiance measurements were performed using an irradiance calibrated AvaSpec-2048–2 spectrometer (Avantes, NL) provided with a 200 µm diameter optical fiber (FC-UVIR200–2 ME, Avantes) and an 8 mm active area cosine corrector (CC-UV–VIS/ NIR, Avantes). The spectrometer operates in the 200 – 1100 nm range (300 lines per mm grating) and is equipped with an AvaBench-75 optical bench, a 25 µm slit which produced 1.2 nm FWHM spectral resolution and a 2048-pixel CCD detector. The total light dose for each textile mock-up, after 203 h, experiments were respectively: $5{,}68\times10^{\circ4}$ Watt*h/m^2 for DGB, $3{,}45\times10^{\circ4}$ Watt*h/m^2 for DGG and $6{,}04\times10^{\circ4}$ Watt*h/m^2 for YLG. The changes induced in the reflectance and colorimetric properties were monitored at different time interval, Table 1. This procedure was applied to all three textiles.

Methods

VIS-NIR reflectance & fluorescence hyperspectral imaging

Visible and near infrared (VIS–NIR) hyperspectral imaging measurements have been performed using a Surface Optics Corporation SOC 710 camera. The system utilizes a whiskbroom line scanner producing a 696 × 520 pixels hypercube in the 400 – 1000 nm spectral range with 128 bands producing an about 4.5 nm spectral step. The camera was positioned at about 1.5 m from the surface obtaining 20 × 30 cm single frames with about 0.4 mm of lateral resolution. Two halogen lamps Elinchrom Scanlite were used as illumination sources (300 W) for reflectance measurements. The sources were placed at 45° and at a 1.5 m distances with respect to the dress. Chemical maps were produced by exploiting the spectral angle mapper algorithm in the ENVI suite.

UV–VIS–NIR reflectance spectroscopy A FieldSpec 4 Hi-Resolution handheld fibre optic spectrometer (ASD) was used

Table 1
Time intervals and corresponding hours and dose light for the different, mock-ups, DGB, DGB and YLG.

Step	Hours (h)	Total light dose (Watt*h/m^2)		
		DGB	DGG	YLG
t0	0	0	0	0
t2	1	$4{,}43\times10^{2} \pm 4.12\times10^{-3}$	$3{,}27\times10^{2} \pm 2.58\times10^{-3}$	$3{,}79\times10^{\circ2} \pm 1.21\times10^{-3}$
t9	8	$4{,}22\times10^{3} \pm 5.81\times10^{-4}$	$2{,}22\times10^{3} \pm 7.27\times10^{-3}$	$3{,}30\times10^{\circ3} \pm 5.89\times10^{-3}$
t12	15	$7{,}25\times10^{3} \pm 1.92\times10^{-3}$	$5{,}01\times10^{3} \pm 7.68\times10^{-4}$	$6{,}29\times10^{\circ3} \pm 2.39\times10^{-3}$
t14	23	$8{,}14\times10^{3} \pm 2.30\times10^{-3}$	$7{,}66\times10^{3} \pm 2.28\times10^{-3}$	$9{,}22\times10^{\circ3} \pm 3.29\times10^{-3}$
t15	29	$9{,}34\times10^{3} \pm 3.90\times10^{-3}$	$9{,}14\times10^{3} \pm 7.88\times10^{-3}$	$1{,}27\times10^{\circ4} \pm 3.34\times10^{-3}$
t16	35	$1{,}16\times10^{4} \pm 1.47\times10^{-2}$	$9{,}73\times10^{3} \pm 5.31\times10^{-3}$	$1{,}46\times10^{\circ4} \pm 1.65\times10^{-3}$
t18	131	$4{,}07\times10^{4} \pm 7.22\times10^{-3}$	$2{,}78\times10^{4} \pm 2.95\times10^{-3}$	$4{,}10\times10^{\circ4} \pm 5.01\times10^{-3}$
t19	203	$5{,}68\times10^{4} \pm 3.17\times10^{-3}$	$3{,}45\times10^{4} \pm 1.73\times10^{-3}$	$6{,}04\times10^{\circ4} \pm 3.07\times10^{-3}$

in-situ and on the mock-ups covering the spectral range 350 – 2500 nm. The instrument is supplied with a 1 m long optical fibre directly connected to the spectrophotometer with a 25° FOV. It is also equipped with two bifurcated fibre optic systems (large and small diameter reflectance probe) which can be connected to the permanent fibre and to an external source with nominal power 12VDC, 30 W. The large diameter reflectance probe (used on the mock-ups) consists of 156 fibres (200 µm), 78 for the excitation and 78 for collecting the reflected light. The large diameter fibre was used with a collection probe for reflected light kept at approximately 20° with respect to the investigated surface (under these conditions, the analysed area was about 6 – 5 mm in diameter). The small diameter reflectance probe (used in-situ on the dress) is composed of 6 illumination fibres (600 µm) surrounding a single collection fibre (600 µm). The distance between the sample and the fibre was kept constant (ca. 1 cm) allowing an area of approximately 2 mm in diameter to be analysed. Spectral resolutions are of 3 nm in the VIS (350 – 1000 nm) and 8 nm in the SWIR (1000 – 2500 nm). White diffuse reference standards were regularly measured using a Spectralon® (Labsphere) tile, reflecting 99 % of the light at each wavelength [33].

Colorimetry Colorimetric measurements of the dress and mock-up textiles were acquired with a Konica-Minolta CM-2600d The experimental conditions are related to the Normal Recommendation 43/93 ("Colorimetric measurements of opaque surface"): spectral range 400 – 700 nm; spherical geometry d:8°; lighting source CIE C; observation angle 10°; reference system CIE L*a*b* colour space; UV radiation contribution not considered; acquisition mode SCE; and spot diameter 3 mm [34]. The ΔE, calculated using the equation, $\Delta E_{1976} = \sqrt{[(\Delta L^*)^2 + (\Delta a^*)^2 + (\Delta b^*)^2]}$, where ΔL^* = lightness-darkness difference, Δa^*= redness-greenness difference, Δb^*= yellowness-blueness difference between t_0-t_x, where t_0 is colorimetric values of dyed textile before irradiation and t_x is the colorimetric values of dyed textile in each irradiation step. All the colorimetric values were acquired in triplicate at each time interval.

External Reflection (ER) mode FTIR spectroscopy All spectra were recorded using a compact portable Bruker Optics ALPHA-R spectrophotometer equipped with a Globar infrared radiation source, a Michelson interferometer (RockSolid (TM)) modified to work in any environmental condition and spatial orientation and a DLaTGS detector. ER mode consents to perform measurements at an angle of incidence at approximately 20°. Spectra were recorded using 186 interferograms across the range 7000 – 375 cm^{-1} with a spectral resolution of 4 cm^{-1}. The correction of background absorption was carried out utilising a reflection spectrum of a reference gold surface. Examined areas observed dimensions of 28 mm^2 [22].

Surface Enhanced Raman Scattering (SERS) Spectra were recorded using a Renishaw inVia confocal micro-Raman spectrometer equipped with solid state diode laser excitation at 532 nm using a 20x objective lens and 1800 gr mm^{-1} grating. SERS measurements were carried out utilising silver colloids. Citrate-reduced colloids were prepared according to the Lee and Meisel procedure [35] by the reduction of silver nitrate (Aldrich 99.9 %) with sodium citrate (Aldrich 99 %). Investigations were carried out by adding a 10 µL drop of colloid aggregated with magnesium sulfate [36] directly onto the textile sample, where spectra could be obtained with 0.05 – 0.1 % of the laser power (0.04 – 0.08 mW) for acquisitions of 3 – 5 s for 3 – 7 accumulations with a spatial resolution of 1 – 2 µm and spectral resolution of 4 cm^{-1}.

Results and discussion

VIS hyperspectral imaging was utilised in-situ in an area of the dress encompassing the less to more faded blue-green areas (Fig. 4.a, i) which permitted the mapping of the distinct patterns (Fig. 4.a, ii-iii) not easily discernible under standard visual conditions. The overall distribution and chemical composition of the different dyestuffs (reds and oranges in Fig. 4.a, ii-iv) reveal insights into the printing production, where each pattern's dye was applied sequentially to the cotton matrix. For example, the VIS reflectance spectra (Fig. 4.b, i-ii) of two different areas (i.e., colours) show the presence of two different dyes. Indeed, the blue-green background has a broad band centred at 618 nm, while the purple has a broad band centred at 582 nm. Thus, the chemical variations permit to individualise and distinguish the dye constituents and mapping their degradation, such as that observed for the purple and blue-green areas given in Fig. 4.a, v-vi. As can be observed by Fig. 4.a, vi, the blue-green background colour presents a progressive degradation, while the purplish hue on the inner circles completely disappears, Fig. 4.a, v.

Aiming to clarify the faded blue-green background coloration, this data was complemented through the micro-destructive analysis of micro-sample. By SERS examination, a characteristic spectral profile (Fig. 4.c) was acquired indicating the likely presence of a triarylmethane dyestuff given by the characteristic SERS marker bands across three key regions: 800 – 1100 cm^{-1} ν_s(CCC)/δ(CCC)breathing/δ(CH$_3$); 1400 – 1500 cm^{-1} (ν_{as}(CCC)/δ(CCC)ring/δ(CH)) and ca. 1600 cm^{-1} (ν(C=C) ring).[37]The ER-FTIR spectra (Fig. 4.d) recorded in a seemingly unfaded area also supported the premise of a triarylmethane over the predominant cotton matrix given by the ν_s(C=C) aromatic band located at 1580 cm^{-1}.

To permit a fuller interpretation of the data collected in-situ, a targeted preparation of cotton mock-ups dyed with selected blue-green triarylmethanes in commerce when the dress was printed were produced. The choice was based on our data base, considering the class of dyes (TAMs), the production's year, the colour hue and the similarity on the UV–VIS spectra in-situ vs our data base. Moreover, it was necessary to focus on the artificial ageing of the mock-ups to provide a better understanding of the degradation phenomenon experienced by the dress which was most likely

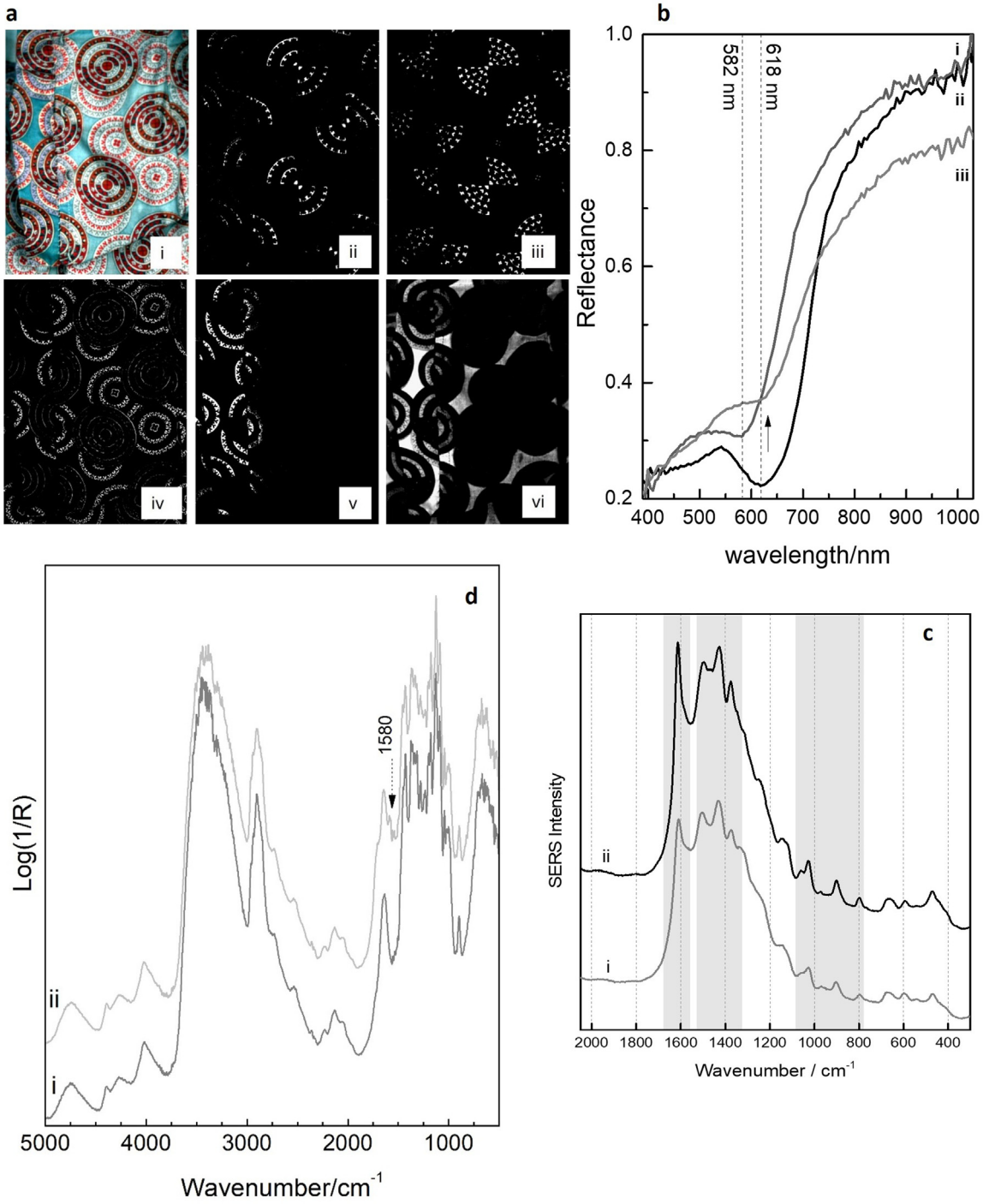

Fig. 4. **a**) VIS hyperspectral mapping images of the dress T.2–1926: i) dress, ii) red dye distribution, iii) orange dye distribution, iv) red and orange, v) purple dye distribution and, vi) blue-green dye distribution; **b**) spectral profiles related to i) purple, areas of the blue-green dye- ii) less faded and iii) more faded; **c**) SERS spectra of two blue-green μ-samples i) more faded and ii) less faded; **d**) ER-FTIR spectra of i) cotton standard and ii) cotton dress on less faded blue-green area.

worn and exposed to natural outdoor light before its later display in a museum environment.

The UV–VIS–NIR reflectance spectra of freshly dyed cotton textiles using triarylmethane dyes, alongside spectra captured during successive controlled photoaging steps can be observed in Fig. 5.a. For simplification in the discussion of results, the designation "t18" will be considered, which corresponds to 4.07×10^4 Watt/m² for DGB, 2.78×10^4 Watt/m² for DGG and 4.10×10^4 Watt/m² for YLG of total light dose, over 131 h of light exposure; and the designation "t19", which corresponds to 5.68×10^4 Watt/m² for DGB, 3.45×10^4 W/m² for DGG, and 6.04×10^4 Watt/m² for YLG of total light dose, over 203 h of light exposure. For the others time intervals and corresponding total light dose, see Table 1 for details in the Experimental Section. As summarised in Table 2, the initial spectral features (t_n) for DGB, DGG, and YLG are similar, with all displaying two distinct reflectance bands in the visible range. The reflectance maxima, however, emphasises structural differences among the dyes: DGB exhibits peaks at 628 nm (with a shoulder at 578 nm) and 431 nm; DGG at 633 nm (with a shoulder at 588 nm) and 431 nm; YLG at 639 nm (with a shoulder at

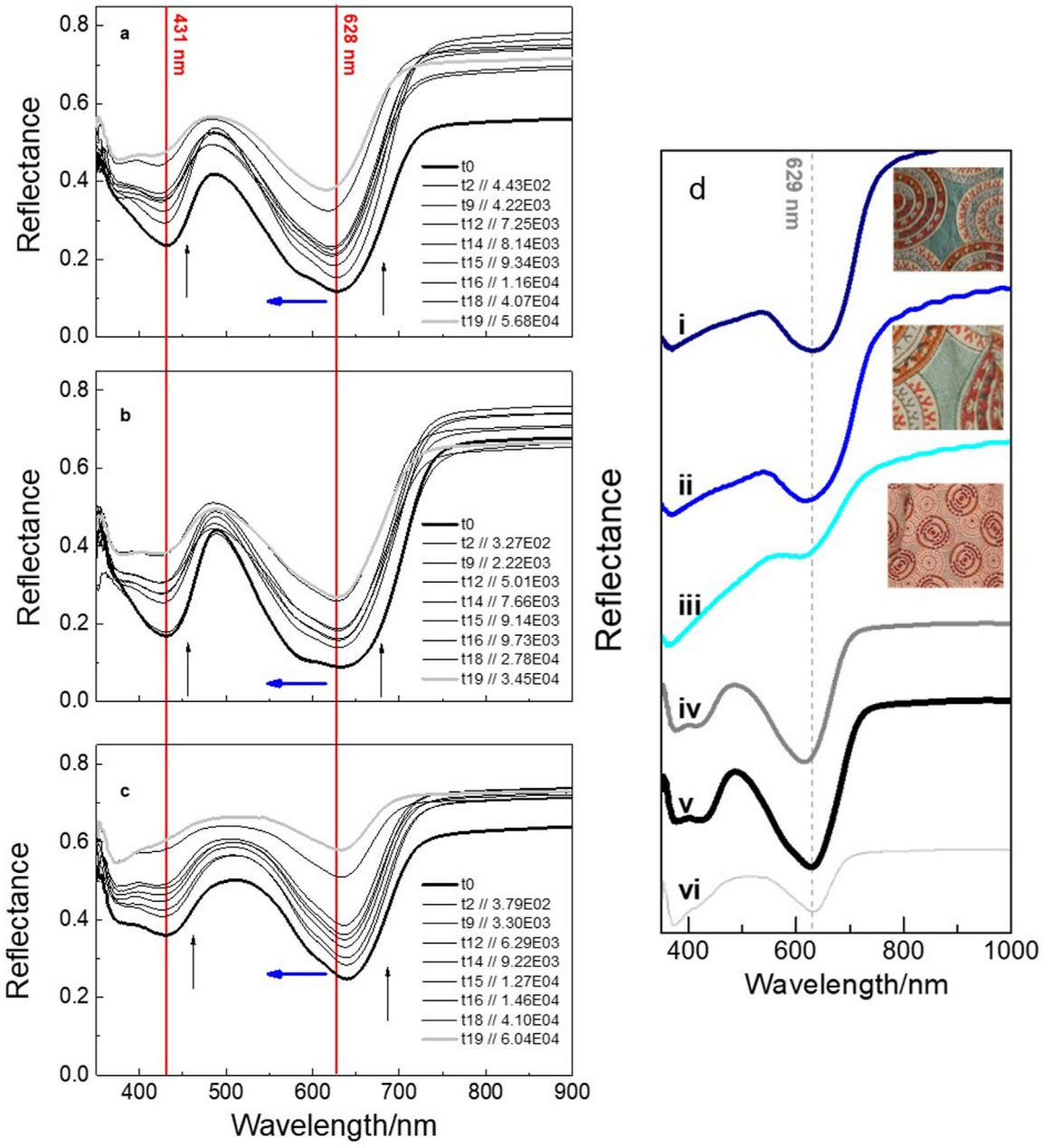

Fig. 5. UV–VIS–NIR reflectance spectra of **a**) DGB, **b**) DGG and **c**) YLG along the artificial aging (t_0 bold black line and different steps of irradiation at grey line, included the respectively total light dose [Watt*h/m^2]). Upon irradiation, a blue shift is observed, signed by blue arrow. The red shift induced by the substitution of heavier functional groups on the three conjugated aromatic is highlighted with the red line; **d**) UV–VIS–NIR reflectance spectra of different areas of dress i.T.2–1926 – dark blue, ii. mid-blue and iii. light blue, iv. DGB; v. DGG and vi. YLG after t19 (last step of aging).

Table 2
Spectral features, the absorption wavelengths (λ_{abs}) of the dyed textiles with DGB, DGG and YLG, at t_0, T18 and T19.

Sample	$\lambda_{abs, t0}$ (nm)	$\lambda_{abs, T18}$ (nm)	$\lambda_{abs, T19}$ (nm)
diamond green B	628	618	617
	578*	-	-
	431	424	424
diamond green G	633	629	629
	588*	580*	580*
	431	431*	431*
yellowish light green SF	639	634	632
	597*	-	-
	431	432*	-

* shoulder.

597 nm) and 431 nm. Thus, it can be hypothesised that the maximum of reflectance at the major wavelengths is indeed attributed to the monomeric form, while the observed shoulder is attributed to the dimeric species. This class of dyes is known to undergo aggregation, with the band at approximately 590 nm attributed to a monomeric species (α-band) and the band at 550 nm associated with a dimeric species (β-band) [18]. The UV–VIS-NIR reflectance spectra of DGG and YLG, in comparison to DGB, exhibit a red shift (see Fig. 5.a, red line). This shift is likely due to a reduction in the energy gap between the HOMO-LUMO orbitals, caused by the substitution of heavier functional groups on the three conjugated aromatic rings. Upon artificial aging, all the textiles showed a decrease in the reflectance intensity of the chromophore band, accompanied by a blue shift (see Fig. 5.a, blue arrow). The blue shift,

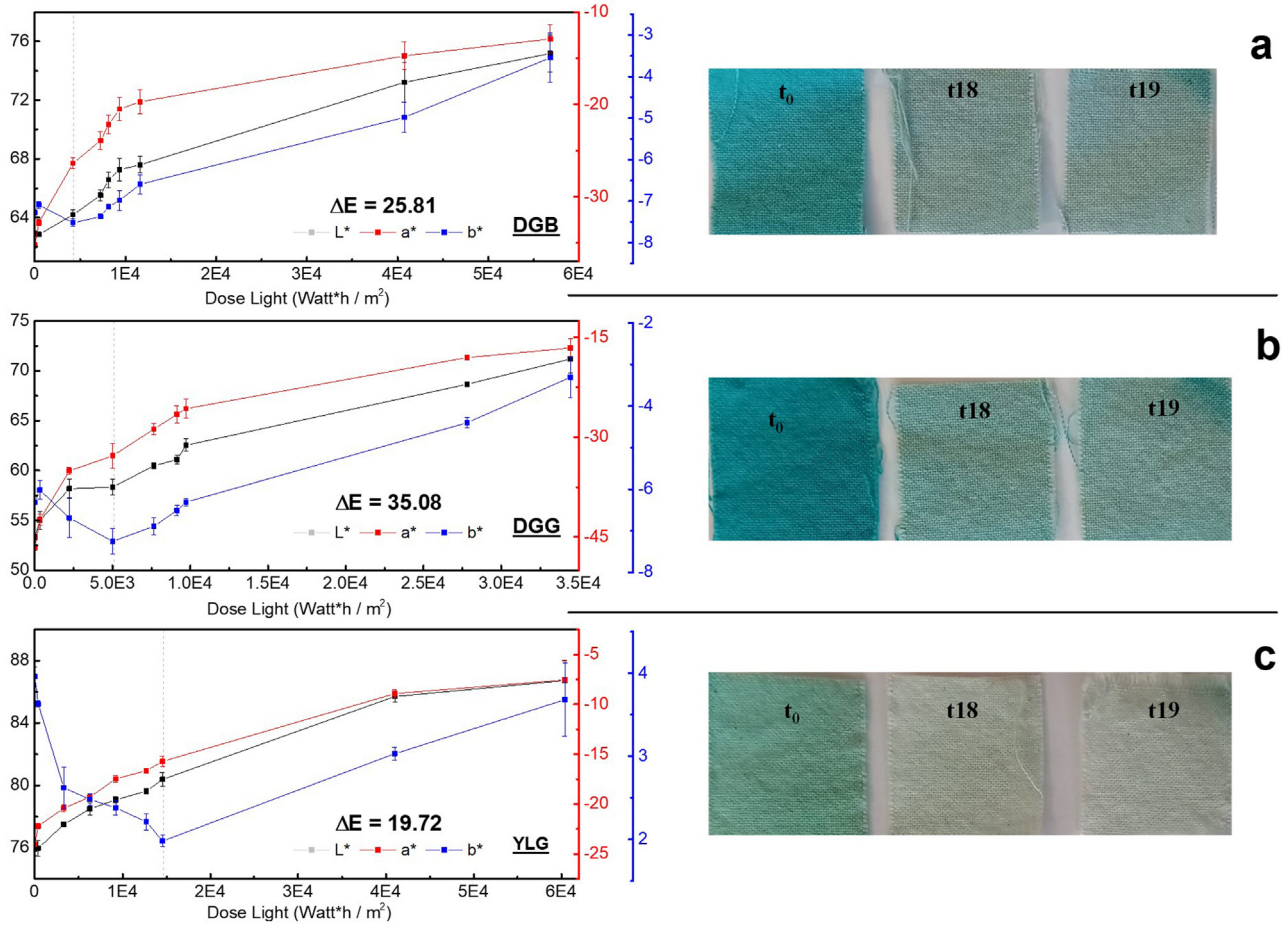

Fig. 6. Colorimetric data and the correspondent dyed textiles images at t_0, t18 and t19 **a**) DGB, **b**) DGG and **c**) YLG on artificial aging.

a characteristic behaviour of triarylmethane dyes [3,17,18], is observed as follows: DGB shows a blue shift of approximately 11 nm (from λ_{abs} = 628 nm to λ_{abs} = 617 nm); DGG exhibits a blue shift of around 4 nm (from λ_{abs} = 633 nm to λ_{abs} = 629 nm); and YLG shows a blue shift of about 7 nm (from λ_{abs} = 639 nm to λ_{abs} = 632 nm) and is a direct consequence of the demethylation process for each dye as the removal of N-substituents groups makes the dye molecule more oxidised, causing it to absorb light at shorter wavelengths, corresponding to higher energy transitions in the molecules.

UV–VIS–NIR reflectance spectra collected from three different areas of the dress representative of differing blue fading hues (T.2–1926: dark blue, blue and light blue) could be directly compared with the photoaged cotton mock-ups of DGB, DGG and YLG – after t19 (last step of aging), Fig. 5.b. The areas of the dress T.2–1926_dark blue, _blue and _light blue, observe a maximum wavelength at, 633 nm, 620 nm and 620 nm, respectively. Spectrally, they appear more similar to DGB and DGG than to YLG (see Table 2). The UV–VIS-NIR reflectance spectra from the cotton mock-ups prepared under a minimal technique of dye with tannin mordant do not perfectly overlap with those from the different regions of the dress accountable for the diverse textile roughness and varied production techniques utilised.

The colorimetric parameters can be observed in Fig. 6 where ΔE was obtained for each cotton mock-up. Tracking the ΔE values provided a means to evaluate the visual fading and degradation of the TAM dyes on cotton. From the dyed textiles under study, YLG present the lower ΔE value, ΔE = 19.72 ± 2.39, and DGG the higher ΔE = 35.08 ± 2.04. In detail, the parameters which influences the ΔE values were both the luminosity (L^*) and green-red component (a^*). In all samples, the L* component values consistently increased under artificial aging, indicating fading and a lighter hue in the textile. Shifts in a* (increasing) and b* (increasing) values reflect changes in hue, transitioning from a greener tone (a*) to a more yellowish one (b*), which aligns with the loss of the dyes' greenish colour. Additionally, the increase in b* values (indicated by the dashed line in Fig. 5) suggests that, at a certain point, the degradation of the dye may reveal the underlying cotton substrate. Indeed, for undyed cotton mock-ups, the colorimetric changes are negligible when compared to those observed in dyed mock-ups. In particular, the colorimetric parameters changed as follow: L* from 87.84 to 90.04, a* from 1.5 to 0.4 and b* from 12.09 to 8.56, which resulted in a ΔE = 4.32 ± 0.50. This ΔE variation is minor when compared to that of the dyed mock-ups. In addition, the UV–VIS reflectance spectrum of the undyed cotton mock-up, characterized by a band centred at approximately 375 nm, does not significantly affect the chromophores' reflectance bands (380 – 450 nm and 540 – 700 nm). Furthermore, after 203 h of artificial ageing, the characteristic cotton band at 375 nm remains unchanged.

External reflection mode FTIR spectra were acquired for undyed cotton and TAM-dyed cotton mock-ups before and after t18 and t19 of irradiation, 131 h and 203 h, respectively (for the correspondent total light dose, Table 1). As shown in the detail in Fig. 7.a for DGG, the characteristic signal at 1580 cm^{-1} is observable where it is noted that the intensity of this band, associated with C=C stretching of a substituted ring (C-Ph-N), disappears after t18 of aging. This behaviour is mirrored for DGB, confirming the presence

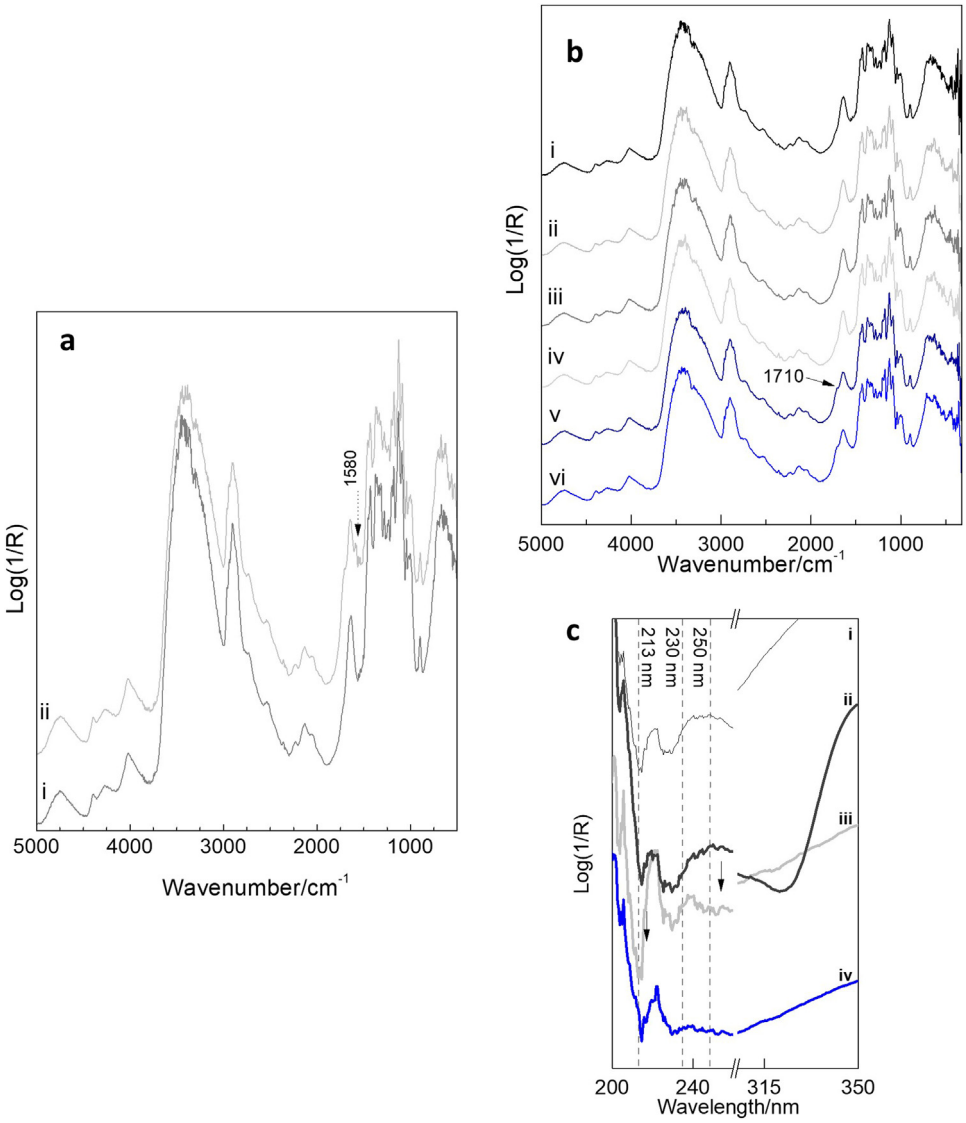

Fig. 7. **a**) ER-FTIR spectra of DGG, at ii. t_0 and i. t18; **b**) ER-FTIR spectra of i. undyed aged cotton, ii. DGB, iii. DGG, iv. YLG after last step of aging (t19) and, points on dress v. T.2–1926 – dark and vi. T.2–1926 – light. All spectra have been normalised and vertically overlayed for clarity; **c**) UV reflectance spectra of i. aged cotton, ii. unaged DGG, iii. aged DGG (t19) and iv. micro-sample dress.

of a TAM in the calico dress [27,37]. The full range ER-FTIR spectra in Fig. 7.b instead compares the aged cotton and its dominant signals, DGB, DGG, and YLG after T19, 203 h of light exposure, with points collected from the dress (T2.1926_02 – dark blue and T2.1926_08 – light blue). Resulting spectra of the dress shows a pronounced shoulder at 1710 cm^{-1}, which is not observed in the TAM dyed cotton prepared herein at the time of aging achieved. A broadening in the 1700 cm^{-1} range is in any case visible in Fig. 7.a. This peak characteristically assigned to υ(C=O), ester carbonyl may be an indicator of residual Michler's ketone, an intermediate in the triarylmethane dye production itself or from the formation of carbonyl functionalities on dye degradation [3,17,18]. However, it is not always straightforward to attribute the presence of dealkylated components to the degradation of the original molecule or to the presence of synthesis by-products [38]. To examine this presence of possible photoproducts non-invasively, the acquisition of spectra below 350 nm on the cotton mock-ups and on the micro-sample dress was conducted (Fig. 7.c). It is possible that the UV bands of benzophenone could be appreciated in the aged DGG (Fig. 7.c, iii) and micro-sample from the dress (Fig. 7.c, iv) at 213 nm, 230 nm and 250 nm over the signals of aged cotton and unaged DGG [39].

The SERS spectra of unaged DGB and DGG mock-ups present marker bands for their differentiation (Fig. 8.a, i; b, i). Specifically, the peaks at 1162 cm^{-1} (νs(CCC)/δ(CCC) breathing/δ_r(CH3)) and 1427 cm^{-1} (δas(CH3)) present in DGG are absent in DG. Spectra for YLG mock-up are not given here since no conventional SERS enhancement could be achieved. It was only on prior hydrolysis could sufficient scattering be observed, contrary to the method for the micro-sample from the dress. Upon irradiation of the dyes on cotton (Fig. 8.a, i-iii; b, i-iii), there is an overall loss of intensity of peaks across the entire spectral range. The decrease in common peaks, evidenced in the grey ranges, specifically at ca. 1340 cm^{-1} and 1590 cm^{-1} indicate a general loss of aromaticity [27,40].

Langer, J. et al., suggests that the consistency of the band at 1366 – 1369 cm^{-1} (phenyl-N stretching) hypothesises a shared adsorption pathway of adsorption of TAM dyes on the SERS-active substrate occurring through the nitrogen atoms linked to the phenyl groups [41]. In this work it is shown that for DGG (Fig. 8.b) this band persists at all stages of ageing, whilst for DGB it is observed in the unaged DGB and is no longer perceived at any successive aging steps. This is indicative of a clear disruption to the phenyl-N-methyl substituent for DGB on ageing and could well indicate a predominant physisorption of the dye on the SERS-active

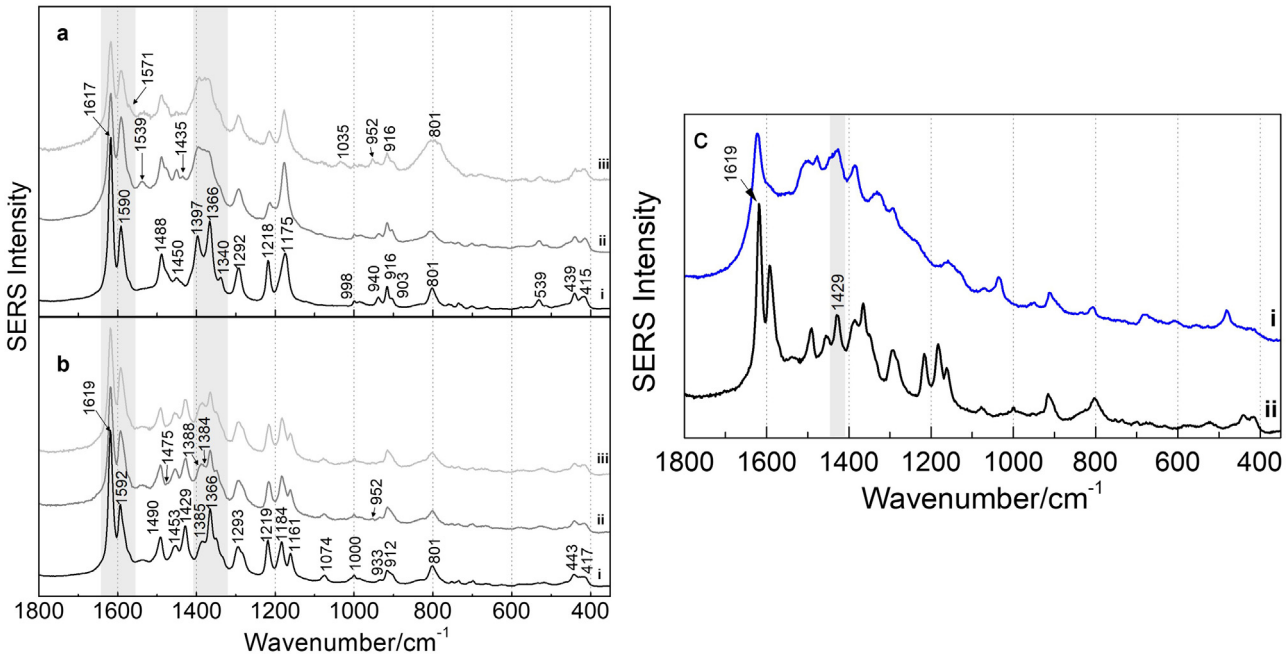

Fig. 8. SERS spectra of **a**) DGB and **b**) DGG mock-ups i. unaged, ii. t18 and iii. t19; **c**) SERS spectra of i. dress sample (T7.1926.01) and ii. DGG mock-up.

substrate [41]. This observation supports the degradation through the N-demethylation pathway where the methyl groups of the dye are sequentially replaced by hydrogen atoms. Notably in DGB, there is a simultaneous increased intensity as degradation progresses of the peak at 804 cm^{-1}, attributed to the NH_2 rocking vibrational motion [42]. The appearance of further peaks on ageing for DGB can be noted, specifically after t18, with peaks at 1435 cm^{-1} attributed to $\delta_{as}(CH_3)$ and 1539 cm^{-1} due to υ(CO) and υ(CC ring). The presence of the carbonyl is significant in relation to the possible formation of photoproducts as aforementioned, noting that its pathway is related to the cleavage of the central C-phenyl bond, leading to benzophenones and phenols as primary degradation products [43]. At t19 instead, very weak peaks for DGB at 952 cm^{-1} γCH(ring), 1035 cm^{-1} δ(CH) and 1571 cm^{-1} can be appreciated. These latter peaks are also present in fuchsine, dye from the same class structurally observing both -CH_3 by -NH_2 groups [2] suggesting the advancement of degradation and chemical modifications on fading. The carbonyl peak at 1539 cm^{-1} is still present with the same relative intensity as previously mentioned.

For DGG, the presence of HSO_4^- counterions although are lost upon dissolution in water, but in the dyeing process they may still influence the initial interaction with the fiber, promoting adsorption and penetration. At t18 of ageing, the peak at 952 cm^{-1} is visible, as well as the 1384 cm^{-1} the 1388 cm^{-1} doublet attributed to $\delta(NCH_3)$ and 1475 cm^{-1} υ(NC ring). No further modifications are observed on ageing to t19, although it is expected that oxidative N-dealkylation shall take place, with eventual replacement of ethyl groups by hydrogen. The comparison of the SERS spectra for DGB and DGG after t19, 203 h of light exposure (see Table 1 for correspondent total light dose), and the micro-sample from the dress (T7.1926.01) highlight a significant overlap between the dress sample and the DGG specifically due to the presence of the peak at 1429 cm^{-1} (Fig. 8.c) which persists across each stage of ageing. This strong correlation supports the recognition of DGG as the main dye utilised in the blue-green areas of the printed cotton dress. The UV–Vis point analyses do not indicate the presence of a dye mixture, as the absorption band profiles are consistent with a single TAM dye. When considered together with the vibrational data, the differences observed between the mock-ups and the dress sample are more plausibly attributed to degradation products than to mixtures of colorants. The SERS spectra of the dress retain the diagnostic features of the TAM family, although the marked spectral broadening suggests a significantly higher degree of degradation than that achieved in the laboratory-aged samples in this work. In the DGB reference, the 1590 cm^{-1} band progressively decreases with ageing, indicating that extended artificial ageing of DGG could similarly lead to its disappearance. The artificial ageing protocol here was intentionally stopped once the colorimetric values matched those of the dress, as the aim was to investigate the spectral characteristics corresponding to that specific colour state.

Conclusions

This study has successfully combined in-situ and laboratory analyses to investigate the fading of the blue-green background in an 1885 printed cotton dress. Non-invasive hyperspectral imaging enabled the mapping of dye distribution and degradation patterns, revealing progressive fading in the blue-green areas. Complementary UV–VIS–NIR reflectance data hinted at the presence of triarylmethane based dyes. Laboratory experiments on artificially aged textile mock-ups dyed with DGG, diamond green B (DGB), and yellowish light green SF (YLG) provided insights into the photofading pathways of TAM dyes. Controlled aging resulted in a characteristic blue shift in reflectance spectra, linked to progressive N-dealkylation and oxidative degradation. SERS analysis of aged samples revealed spectral changes indicative of aromatic ring disruption and the formation of photoproducts, including benzophenone derivatives. Micro-destructive SERS and FTIR analyses confirmed that the background coloration was likely achieved using a triarylmethane (TAM) dye, with spectral markers supporting the presence of diamond green G (DGG). The comparison between artificially aged samples and the dress fabric established a strong correlation between the degradation pathways of DGG and the fading observed in the historical textile. Overall, although the converging spectroscopic evidence points to DGG as the most plausible dye, targeted micro-destructive analyses will be essential to confirm this attribution and should form a key focus of future work.

The results provide valuable data for understanding TAM dye stability in historical textiles that may inform conservation strategies for similar artifacts. By comparing in situ observations with

reference materials subjected to controlled ageing, this work offers interpretative elements that may inform modelling of colour change, while acknowledging the limitations of a non-invasive analytical approach, and supports the development of preventive conservation strategies for TAM-dyed objects in museum collections. Although this recommendation is necessarily qualitative, it is advised to minimize the exposure of TAM-dyed textiles in museum collections to both natural and artificial light. This can be achieved either by using neutral-density filters or by adjusting the lighting system.

Acknowledgements

Authors acknowledge the Mobile Laboratory MOLAB of the Italian node of E-RIHS, European Research Infrastructure for Heritage Science (MUR FOE E-RIHS IT and PON Ricerca e Innovazione 2014–2020, CCI: 2014IT16M2OP005). The European project PERCEIVE Perceptive Enhanced Realities of Coloured Collections through AI and Virtual Experiences (GA Nr. 101061157) and the Project PE 0000020 CHANGES - CUP: B53C22003890006, NRP Mission 4 Component 2 Investment 1.3, Funded by the European Union - NextGenerationEU" under the Italian Ministry of University and Research (MUR).

References

[1] A. Ferretti, E. Floris, B. Campanella, I. Degano, S. Legnaioli, Welcome to the jungle": TLC-SERS to wade through real complex mixtures of synthetic dyes, Microchem. J. 206 (2024) 111439.
[2] A. Cesaratto, J.R. Lombardi, M. Leona, Tracking photo-degradation of triarylmethane dyes with surface-enhanced raman spectroscopy, J. Raman Spectrosc. 48 (3) (2017) 418–424.
[3] G. Favaro, D. Confortin, P. Pastore, M. Brustolon, Application of LC-MS and LC-MS-MS to the analysis of photo-decomposed crystal violet in the investigation of cultural heritage materials aging, J. Mass Spectrom. 47 (12) (2012) 1660–1670.
[4] J. Tierney, From Design to Consumption: The Export Trade in Printed and Dyed Textiles to British West Africa, c.1870-1914, University of Warwick, 2019.
[5] T. Kusamitsu, British Industrialisation and Design 1830-1851, University of Sheffield, 1982.
[6] Edmund Potter (1802-1883). https://glossopheritage.co.uk/ghtarchive/edmundpotter/ (accessed 06 May).
[7] D. Greysmith, The Printed Textiles Industry in England 1830-1870, Middlesex University, 1985.
[8] A. Sansone, The Printing of Cotton Fabrics, Abel Heywood & Son, 1887.
[9] Society of, D.; Colourists; American Association of TextileSociety of Dyers and Colourists C.; Colorists, *Colour index*. 3d ed. ed.; [Bradford, Yorkshire, England], Bradford, Yorkshire, England, 1971 [c1971-]:]p v.
[10] G.S. Egerton, A.G. Morgan, The photochemistry of dyes II—Some aspects of the fading process, J. Soc. Dye. Colour. 86 (6) (1970) 242–249.
[11] C.-C. Chen, F.-D. Mai, K.-T. Chen, C.-W. Wu, C.-S. Lu, Photocatalyzed N-de-methylation and degradation of crystal violet in titania dispersions under UV irradiation, Dyes Pigments 75 (2) (2007) 434–442.
[12] A.L. Henderson, T.C. Schmitt, T.M. Heinze, C.E. Cerniglia, Reduction of malachite green to leucomalachite green by intestinal bacteria, Appl. Environ. Microbiol. 63 (10) (1997) 4099–4101.
[13] D. Tamburini, F. Sabatini, S. Berbers, M.R. van Bommel, I. Degano, An introduction and recent advances in the analytical study of early synthetic dyes and organic pigments in cultural heritage, Heritage 7 (4) (2024) 1969–2010.
[14] M.V. Adamos, W.D.A. Rickard, W. van Bronswijk, G. Sauzier, In-situ profiling of pen ink degradation on paper using raman spectroscopy and ToF-SIMS, Appl. Surf. Sci. 705 (2025) 163500.
[15] S.V.J. Berbers, A.N.P. Gaibor, F. Ligterink, J.G. Neevel, B. Reissland, I.D. van der Werf, Shades of violet: study of the compositional variability of historical Methyl violet dyes, J. Cult. Herit. 66 (2024) 464–475.
[16] M. Anghelone, V. Stoytschew, D. Jembrih-Simbürger, M. Schreiner, Spectroscopic methods for the identification and photostability study of red synthetic organic pigments in alkyd and acrylic paints, Microchem. J. 139 (2018) 155–163.
[17] F. Sabatini, I. Degano, M. van Bommel, Investigating the in-solution photodegradation pathway of Diamond Green G by chromatography and mass spectrometry, Color. Technol. 137 (5) (2021) 456–467.
[18] C. Daria, N. Han, B. Marina, F. Lorenzo, J.K. Albert, M.W. Renè, R.v.B. Maarten, Crystal violet: study of the photo-fading of an early synthetic dye in aqueous solution and on paper with HPLC-PDA, LC-MS and FORS, J. Phys.: Conf. Ser. 231 (1) (2010) 012011.
[19] S. Hisaindee, M.A. Meetani, M.A. Rauf, Application of LC-MS to the analysis of advanced oxidation process (AOP) degradation of dye products and reaction mechanisms, TrAC Trends Anal. Chem. 49 (2013) 31–44.
[20] D. Saviello, M. Trabace, A. Alyami, A. Mirabile, P. Baglioni, R. Giorgi, D. Iacopino, Raman spectroscopy and surface enhanced Raman scattering (SERS) for the analysis of blue and black writing inks: identification of dye content and degradation processes, Front. Chem. (2019) Volume 7 - 2019.
[21] S. Nakagawa, K. Sakakibara, H. Gotoh, Novel degradation mechanism for triarylmethane dyes: acceleration of degradation speed by the attack of active oxygen to halogen groups, Dyes Pigments 124 (2016) 130–132.
[22] B. Doherty, M. Vagnini, K. Dufourmantelle, A. Sgamellotti, B. Brunetti, C. Miliani, A vibrational spectroscopic and principal component analysis of triarylmethane dyes by comparative laboratory and portable instrumentation, Spectrochim. Acta A: Mol. Biomol. Spectrosc. 121 (2014) 292–305.
[23] C. Weyermann, D. Kirsch, C. Costa Vera, B. Spengler, Evaluation of the photodegradation of crystal violet upon light exposure by mass spectrometric and spectroscopic methods, J. Forensic Sci. 54 (2) (2009) 339–345.
[24] C. Weyermann, D. Kirsch, C. Costa-Vera, B. Spengler, Photofading of ballpoint dyes studied on paper by LDI and MALDI MS, J. Am. Soc. Mass Spectrom. 17 (3) (2006) 297–306.
[25] C. Montagner, M. Bacci, S. Bracci, R. Freeman, M. Picollo, Library of UV–Vis–NIR reflectance spectra of modern organic dyes from historic pattern-card coloured papers, Spectrochim. Acta A: Mol. Biomol. Spectrosc. 79 (5) (2011) 1669–1680.
[26] F. Casadio, M. Leona, J.R. Lombardi, R. Van Duyne, Identification of organic colorants in fibers, paints, and glazes by surface enhanced raman spectroscopy, Acc. Chem. Res. 43 (6) (2010) 782–791.
[27] L. Ayed, J. Cheriaa, N. Laadhari, A. Cheref, A. Bakhrouf, Biodegradation of crystal violet by an isolatedBacillus sp, Ann. Microbiol. 59 (2) (2009) 267–272.
[28] D. Tamburini, J. Dyer, C. Cartwright, A. Green, Changes in the production materials of Burmese textiles in the nineteenth century—Dyes, mordants and fibres of Karen garments from the British Museum's collection, Herit. Sci. 11 (1) (2023) 150.
[29] D.-J. Cao, J.-J. Wang, Q. Zhang, Y.-Z. Wen, B. Dong, R.-J. Liu, X. Yang, G. Geng, Biodegradation of triphenylmethane dye crystal violet by Cedecea davisae, Spectrochim. Acta A: Mol. Biomol. Spectrosc. 210 (2019) 9–13.
[30] A. Ferretti, I. Degano, S. Legnaioli, B. Campanella, A. Sainati, M.P. Colombini, Shedding light on the composition and degradation mechanism of dyes in historical ink's collection (19th-20th century), Dyes Pigments 220 (2023) 111672.
[31] Museum, V.A. Dress. https://collections.vam.ac.uk/item/O122400/dress-unknown/.
[32] Stephen A.C. Bowes, Shannon Elliott, La Tasha Harris, Laura Hazlett, Ester Méthé, Muhammadin Razak, Pugi Yosep Subagiyo, Important Early Dynthetic Dyes. Chemistry, Constitution, Date, Properties. Conservation Analytical Laboratory Smithsonian Institution, 1991.
[33] F. Pottier, S. Kwimang, A. Michelin, C. Andraud, F. Goubard, B. Lavédrine, Independent macroscopic chemical mappings of cultural heritage materials with reflectance imaging spectroscopy: case study of a 16th century Aztec manuscript, Anal. Methods 9 (42) (2017) 5997–6008.
[34] G. Germinario, S. Garrappa, V. D'Ambrosio, I.D. van der Werf, L. Sabbatini, Chemical composition of felt-tip pen inks, Anal. Bioanal. Chem. 410 (3) (2018) 1079–1094.
[35] P.C. Lee, D. Meisel, Adsorption and surface-enhanced Raman of dyes on silver and gold sols, J. Phys. Chem.; (U. S.) 86 (1982) 3391–3395 17, Medium: X; Size: Pages.
[36] S.E.J. Bell, N.M.S. Sirimuthu, Surface-enhanced raman spectroscopy (SERS) for sub-micromolar detection of DNA/RNA mononucleotides, J. Am. Chem. Soc. 128 (49) (2006) 15580–15581.
[37] K. Mardenborough, M. Florentino, R. Haxhari, Y.-C. Lin, M. Rafailovich, G. Halada, H.J. Jung, T. Kim, Influence of NaOH concentration on the decolorization of crystal violet dyed cotton fabric, Environ. Eng. Res. 28 (2023) 210643.
[38] D. Tamburini, On the reliability of historic books as sources of reference samples of early synthetic dyes – the case of "the coal tar colours of the farbwerke vorm. Meister, Lucius & Brüning, Höchst on the Main, Germany – a general part" (1896), Dyes Pigments 221 (2024) 111796.
[39] B. Rånby, W. Yang, O. Tretinnikov, Surface photografting of polymer fibers, films and sheets, Nucl. Instrum. Methods Phys. Res. B-beam Interact. Mater. At. - Nucl. Instrum. Meth. Phys. Res. B 151 (1999) 301–305.
[40] R. de Oliveira, A.C. Sant'Ana, Crystal violet degradation by visible light-driven AgNP/TiO2 hybrid photocatalyst tracked by SERRS spectroscopy, Vib. Spectrosc. 133 (2024) 103694.
[41] J. Langer, D. Jimenez de Aberasturi, J. Aizpurua, R.A. Alvarez-Puebla, B. Auguié, J.J. Baumberg, G.C. Bazan, S.E.J. Bell, A. Boisen, A.G. Brolo, J. Choo, D. Cialla-May, V. Deckert, L. Fabris, K. Faulds, F.J. García de Abajo, R. Goodacre, D. Graham, A.J. Haes, C.L. Haynes, C. Huck, T. Itoh, M. Käll, J. Kneipp, N.A. Kotov, H. Kuang, E.C. Le Ru, H.K. Lee, J.-F. Li, X.Y. Ling, S.A. Maier, T. Mayerhöfer, M. Moskovits, K. Murakoshi, J.-M. Nam, S. Nie, Y. Ozaki, I. Pastoriza-Santos, J. Perez-Juste, J. Popp, A. Pucci, S. Reich, B. Ren, G.C. Schatz, T. Shegai, S. Schlücker, L.-L. Tay, K.G. Thomas, Z.-Q. Tian, R.P. Van Duyne, T. Vo-Dinh, Y. Wang, K.A. Willets, C. Xu, H. Xu, Y. Xu, Y.S. Yamamoto, B. Zhao, L.M. Liz-Marzán, Present and future of surface-enhanced Raman scattering, ACS Nano 14 (1) (2020) 28–117.
[42] T.E. Tesema, B. Kafle, M.G. Tadesse, T.G. Habteyes, Plasmon-enhanced resonant excitation and demethylation of methylene blue, J. Phys. Chem. C 121 (13) (2017) 7421–7428.
[43] M. Sowula, T. Misiaszek, W. Bartkowiak, Solvent effect on the vibrational spectrum of Michler's ketone. Experimental and theoretical investigations, Spectrochim. Acta A: Mol. Biomol. Spectrosc. 131 (2014) 678–685.